NEOPLASIA
www.neoplasia.com

Volume 15 Number 5 May 2013 pp. 535–543 535

Inhibition of SUR1 Decreases the Vascular Permeability of Cerebral Metastases[1]

Eric M. Thompson*, Gregory L. Pishko†, Leslie L. Muldoon† and Edward A. Neuwelt*,†,‡

*Department of Neurological Surgery, Oregon Health & Science University, Portland, OR; †Department of Neurology, Oregon Health & Science University, Portland, OR; ‡Department of Veterans Affairs Medical Center, Portland, OR

Abstract

Inhibition of sulfonylurea receptor 1 (SUR1) by glyburide has been shown to decrease edema after subarachnoid hemorrhage. We investigated if inhibiting SUR1 reduces cerebral edema due to metastases, the most common brain tumor, and explored the putative association of SUR1 and the endothelial tight junction protein, zona occludens-1 (ZO-1). Nude rats were intracerebrally implanted with small cell lung carcinoma (SCLC) LX1 or A2058 melanoma cells ($n = 36$). Rats were administered vehicle, glyburide (4.8 μg twice, orally), or dexamethasone (0.35 mg, intravenous). Blood-tumor barrier (BTB) permeability (K^{trans}) was evaluated before and after treatment using dynamic contrast-enhanced magnetic resonance imaging. SUR1 and ZO-1 expression was evaluated using immunofluorescence and Western blots. In both models, SUR1 expression was significantly increased ($P < .05$) in tumors. In animals with SCLC, control mean K^{trans} (percent change ± standard error) was 101.8 ± 36.6%, and both glyburide (−21.4 ± 14.2%, $P < .01$) and dexamethasone (−14.2 ± 13.1%, $P < .01$) decreased BTB permeability. In animals with melanoma, compared to controls (117.1 ± 43.4%), glyburide lowered BTB permeability increase (3.2 ± 15.4%, $P < .05$), while dexamethasone modestly lowered BTB permeability increase (63.1 ± 22.1%, $P > .05$). Both glyburide ($P < .001$) and dexamethasone ($P < .01$) decreased ZO-1 gap formation. By decreasing ZO-1 gaps, glyburide was at least as effective as dexamethasone at halting increased BTB permeability caused by SCLC and melanoma. Glyburide is a safe, inexpensive, and efficacious alternative to dexamethasone for the treatment of cerebral metastasis–related vasogenic edema.

Neoplasia (2013) 15, 535–543

Introduction

Metastases are by far the most common type of brain tumor with an annual incidence of more than 200,000 [1] in the United States, approximately 10 times that of malignant primary brain tumors [2]. At least 10% [1] of adults with cancer develop symptomatic cerebral metastases and incidence continues to rise [3,4] due to improved systemic control and improved imaging detection. Cerebral metastases cause significant edema and mass effect in 33% of patients [5] resulting in decreased quality of life due to neurological deficits and headache.

By decreasing tumor vascular permeability [6–8], glucocorticoids are the mainstay treatment of edema caused by cerebral metastases [9]. However, glucocorticoid use is associated with a multitude of dose- and time-dependent adverse side effects such as immunosuppression and endocrinopathies [10]. Newer vascular targeting agents such as bevacizumab, a monoclonal antibody targeting vascular endothelial

Abbreviations: BTB, blood-tumor barrier; DCE-MRI, dynamic contrast-enhanced magnetic resonance imaging; NIH, National Institutes of Health; NS, 0.9% NaCl; OHSU, Oregon Health & Science University; SAH, subarachnoid hemorrhage; SCLC, small cell lung carcinoma; SUR1, sulfonylurea receptor 1; VEGF, vascular endothelial growth factor; ZO-1, zona occludens-1

Address all correspondence to: Edward A. Neuwelt, MD, Department of Neurology, Blood-Brain Barrier Program, Oregon Health & Science University, 3181 SW Sam Jackson Parkway Road, L603, Portland, OR 97239. E-mail: neuwelte@ohsu.edu

[1]This study was supported by a Medical Research Foundation of Oregon Early Clinical Investigator grant to E.M.T. and by a Veterans Administration merit review grant and by National Institutes of Health grants NS053468, CA137488, and NS44687 to E.A.N. No author has any conflict of interest to disclose.

Received 9 January 2013; Revised 4 March 2013; Accepted 11 March 2013

DOI 10.1593/neo.13164

growth factor (VEGF), also rapidly decrease brain tumor permeability [11,12] and tumor-associated edema in malignant gliomas [13,14] but are cost prohibitive for many patients [15]. The need for a safe, inexpensive, novel agent that effectively decreases blood-tumor barrier (BTB) permeability and reduces vasogenic edema is of paramount importance.

Sulfonylurea receptor 1 (SUR1) is a subunit that regulates the activity of adenosine triphosphate (ATP)-sensitive potassium channels and the ATP/Ca^{2+} nonselective cation channel [16]. SUR1 is upregulated in neurons, astrocytes, and capillary endothelial cells following ischemic stroke [17] and in neurons and endothelial cells in brain contusions [18] and post–subarachnoid hemorrhage (SAH) inflammation [19]. The mechanism for glyburide activity in SAH appears to involve rearrangement of zona occludens-1 (ZO-1), a key protein of the endothelial tight junction complex, and subsequent decreased vasogenic edema, possibly by decreasing endothelial cytotoxic injury.

Glyburide is a potent SUR1 inhibitor [17] frequently used to treat type II diabetes mellitus and has a minimal side effect profile consisting primarily of hypoglycemia [20]. Glyburide has been reported to decrease stroke volume, post-stroke cerebral edema, and mortality following ischemic stroke [17], decrease microvascular fragmentation and hemorrhage following traumatic brain contusion [18], and decrease vasogenic edema SAH [19]. Because the blood-brain barrier is leaky in cerebral metastases, we hypothesized that the expression of SUR1 is increased and glyburide might decrease BTB permeability.

The primary objective of this study was to determine if SUR1 is expressed in metastatic brain tumors in animal models and, if so, to determine if inhibiting SUR1 with glyburide is effective in decreasing BTB permeability as determined by dynamic contrast-enhanced magnetic resonance imaging (DCE-MRI). DCE-MRI evaluates the permeability of vessels using the measures transfer coefficient (K^{trans}) and extravascular extracellular space volume fraction (v_e). In an intact blood-brain barrier, $K^{trans} \approx 0$ min^{-1} [21,22] and v_e is unmeasurable because v_e can only be measured when contrast leaks from the vessels to the extravascular extracellular space [23]. The secondary objectives were to evaluate a putative relationship between SUR1 and ZO-1 and to determine if glyburide improves survival in brain tumor models. Our results demonstrate that glyburide is a well-tolerated novel therapy for decreasing the vasculature permeability of cerebral metastases.

Materials and Methods

Tumor Implantation

All procedures were approved by the Oregon Health & Science University (OHSU) Institutional Animal Care and Use Committee. LX1 human small cell lung carcinoma (SCLC) cells (obtained from Mason Research Institute, Worcester, MA) were cultured in RPMI 1640 with 10% FBS and antibiotics. UW28 human malignant glioma cells (courtesy of Dr Ali-Osman, Duke University, Durham, NC) and A2058 human melanoma cells (ATCC, Manassas, VA) were grown in Dulbecco's modified Eagle's medium with 10% FBS and antibiotics. Nude rats (rnu/rnu) from the OHSU colony were sedated and underwent stereotactic cell injection into right basal ganglia (BG; 3.2 mm lateral to the bregma at a depth of 6.2 mm) as previously described [11].

Dynamic Contrast-Enhanced Magnetic Resonance Imaging

The initial (pretreatment) DCE-MRI was performed after intracerebral cell implantation on day 7 for the LX1 group, days 9 and 10 for the A2058 group, and day 14 for the UW28 group. The second (posttreatment) DCE-MRI was performed 48 hours later. Animals were sedated and monitored during the MRI sessions in an (11.75 T) MRI instrument (Bruker, Billerica, MA) as previously described [24]. Throughout the imaging session, warm air was continuously blown through the bore to keep the animals' body temperature between 35.5 and 37°C.

High-resolution rapid acquisition with refocused echo axial T2-weighted images (repetition time/echo time = 4020 ms/12 ms, rapid acquisition with refocused echo factor = 8, field of view = 3.2 × 3.2 cm^2, slice thickness = 1 mm, 25 slices, matrix = 256 × 256, one average) was obtained and used to select the slice with the largest tumor area to plan the DCE-MRI. Precontrast T1 value (T10) in tumor was determined as previously described [24]. The DCE-MRI was performed using a previously described inversion recovery sequence [24] using 0.1 mM/kg gadodiamide. Precontrast and postcontrast high-resolution T1-weighted images were acquired using a fast low-angle shot sequence for tumor area measurements (repetition time/echo time = 160 ms/1.6 ms, field of view = 3.2 × 3.2 cm^2, slice thickness = 1 mm, 25 slices, matrix = 256 × 256, four averages). Animals were stratified into treatment groups (n = 6 per group) based on pretreatment high-resolution coronal T2-weighted tumor size. Following the DCE-MRI session, sedation was reversed using 1.25 mg of atipamezole hydrochloride (Zoetis, Florham Park, NJ).

Tumor Permeability and Size Calculation

All DCE-MRI data fitting and pharmacokinetic modeling was performed using a nonlinear least squares method with an OHSU in-house software package written in MATLAB (MathWorks, Inc, Natick, MA). Animal-specific arterial input function was based on the superior sagittal sinus. Amplitude of the arterial input function was adjusted for each DCE-MRI experiment using the reference tissue (temporalis muscle) method [24]. Tumor-specific, volume-averaged T10 values measured from the inversion recovery (IR) sequence were used in the analysis. Standard Toft's two-compartment model [25] was used for all cases to fit K^{trans} and v_e.

Each tumor region of interest was selected by a single author (E.M.T.). Pixel-by-pixel DCE fast exchange limit maps were calculated. Because the pixel-by-pixel maps demonstrated non-normally distributed K^{trans} and v_e in the tumor region of interest, the median values of each were calculated using an OHSU software package written in MATLAB (MathWorks, Inc).

The coronal slice with the largest tumor area as demonstrated on high-resolution T2-weighted MRI was measured using ImageJ [National Institutes of Health (NIH)]. Tumor area was also measured on the analogous slices in precontrast and postcontrast T1-weighted MRI. Animals with tumors < 0.1 cm^2 were excluded from permeability analysis.

Medication Administration

Animals were administered vehicle, glyburide, or dexamethasone after the pretreatment DCE-MRI. A 5-mg glyburide tablet was suspended in 5 ml of DMSO. One milliliter of this solution was then suspended in 100 ml of 0.9% NaCl (NS) creating a glyburide suspension of 1 mg/100 ml. The vehicle was prepared by suspending 1 ml of DMSO in 100 ml of NS. The day following the pretreatment DCE-MRI, animals were administered either 4.8 μg of glyburide or 480 μl of

vehicle twice 8 hours apart through oral gavage or a single dose of IV dexamethasone (0.35 mg) administered through the tail vein.

Following the posttreatment DCE-MRI, a subcutaneous pump was implanted to deliver continuous treatment. A glyburide tablet (5 mg) was dissolved in 1 ml of DMSO and then diluted in 11.5 ml of NS. To prepare the vehicle, 1 ml of DMSO was added to 11.5 ml of NS. Dexamethasone tablets (24 mg) were dissolved in 1 ml of DMSO and then diluted in 3 ml of NS. These dilutions yielded a glyburide delivery of 400 ng/hour and dexamethasone delivery of 3 μg/hour. Following the posttreatment DCE-MRI, a small incision was made between the scapulae, and a pump (0.5 μl/hour, Alzet model 2002) filled with vehicle, glyburide, or dexamethasone was placed subcutaneously. Approximately 7 hours following the first medication administration and 24 hours following subcutaneous pump implantation, animals were sedated using isoflurane and a small lancet was used to pierce a dorsal metatarsal vein. The serum glucose when evaluated using an ACCU-CHEK glucometer. Animals were followed for survival and were examined at least every 2 days. Animals were sacrificed if they demonstrated severe neurologic deficit or >20% weight loss.

Immunofluorescence

Animals were killed by intraperitoneal injection with 20 mg of pentobarbital and intracardiac perfusion of NS. Brains were flash frozen, cryostat sectioned at 9 μm, and fixed in 4% formalin. Immunohistochemistry was performed using goat anti-SUR1 (Santa Cruz Biotechnology, Dallas, TX) and rabbit anti–ZO-1 (Life Technologies, Carlsbad, CA) at 1:200 dilutions. Slides were then incubated in species-specific fluorescent antibodies (Life Technologies) for 60 minutes, washed with phosphate-buffered saline, and then incubated in 4′,6-diamidino-2-phenylindole(Life Technologies) for 1 minute.

Six random high-powered fields (×200) from at least two histologic sections of both the tumor and the contralateral BG were photographed using standardized acquisition. Area of fluorescence was quantified using ImageJ (NIH). Disruption of ZO-1 was quantified using ×400 images of six intratumoral vessels per animal. ImageJ (NIH) was used to measure the total percentage of gap in the ZO-1 fluorescence for each vessel. To assess the presence SUR1 and ZO-1 constitutive expression in LX1 and A2058 cells *in vitro*, 1×10^5 of each cell type was grown overnight in a six-well plate. The cells were prepared for immunofluorescence using the aforementioned methods. All specimens were visualized on Zeiss Axioplan microscope using a Zeiss Axiocam camera.

Western Blot Analysis

Animals were killed by intraperitoneal injection with 20 mg of pentobarbital and intracardiac perfusion of NS. The brains were removed, and approximately 150-mg samples of tumor and normal contralateral BG were excised, homogenized in radioimmunoprecipitation assay buffer containing protease inhibitors, and frozen at −80°C. Samples were then thawed, sonicated, and centrifuged at 14,000 rpm for 20 minutes at 4°C. The supernatants were collected and proteins were separated by electrophoresis, transferred, and blocked as previously described [26]. Primary antibodies used were goat anti-SUR1 (1:500; Santa Cruz Biotechnology), rabbit anti–ZO-1 (1:1000; Life Technologies), or mouse anti-NeuN (1:1000; EMD Millipore, Billerica, MA). The next day, membranes were washed three times in tris-buffered saline with Tween20 (TBST) incubated for 1.5 hours with appropriate HRP-conjugated secondary antibodies, and washed three more times in TBST. The targeted antigens were visualized using standard enhanced chemiluminescence methods (Amersham ECL) and X-ray film. SUR-1 and ZO-1 bands were normalized to NeuN. To semiquantify target protein expression, blot images of at least three animals per treatment group for both metastatic models were analyzed using Un-Scan-It (Silk Scientific, Orem, UT).

Statistical Analysis

All statistical analyses were performed using Prism 4.0 (GraphPad Software, Inc, La Jolla, CA). Permeability (K^{trans} and v_e), SUR1 expression, and ZO-1 disruption were compared for each of the three treatment groups using analysis of variance with Tukey post hoc comparisons. Protein expression of tumoral *versus* contralateral BG was made using a two-tailed non-paired Student's *t* test. Association between tumor permeability, size, change in permeability, and survival was made using Pearson correlation coefficient (r), and survival was compared using a chi-square log rank test.

Results

SUR1 Is Overexpressed in Cerebral Metastases

The constitutive expression of SUR1 in the rodent brain varies with anatomic location with relatively little expression in the BG [27]. The first step was to confirm that SUR1 expression was increased by cerebral metastases and thus amenable to inhibition with glyburide. First, we established that neither cell line constitutively expressed SUR1 *in vitro*. LX1 and A2058 cells had no immunofluorescent activity for SUR1 compared to rodent brain specimens with known SUR1 expression ($P < .01$). Next, we determined that SUR1 expression was significantly increased ($P < .05$) in the tumor regions of both SCLC and melanoma models compared to the contralateral BG where there was little constitutive expression (Figure 1, *A*,–*C*). SUR1 was expressed in the pericellular areas of tumor cells (Figure 1*A*) in glial and endothelial cells. In both metastatic models, there was no difference in SUR1 expression when the three treatment groups were compared using analysis of variance ($P > .05$). Tumor region SUR1 overexpression was supported by Western blot data (Figure 1, *D* and *E*).

Inhibition of SUR1 Decreases the BTB Permeability of Cerebral Metastases

We sought to determine if inhibiting SUR1 with glyburide would decrease BTB permeability and, if so, how this decrease in permeability compared to the decrease in permeability conferred by the standard treatment of tumor-related vasogenic edema, dexamethasone [9]. Vehicle served as the negative control, dexamethasone served as the positive control, and glyburide served as the experiment. To eliminate selection bias, we established that there was no difference in pretreatment (baseline) T2-weighted or post-gadodiamide T1-weighted MRI tumor area, K^{trans}, or v_e between the three treatment groups in either metastatic tumor model ($P > .05$). Importantly, there was also no difference in serum glucose measurements between the three groups and no animal had a serum glucose less than 100 mg/dl (normal 82–187 mg/dl [28]) after treatment with either glyburide or dexamethasone.

As expected, permeability of BTB as determined by K^{trans} of animals in the control group increased by approximately 100% in both

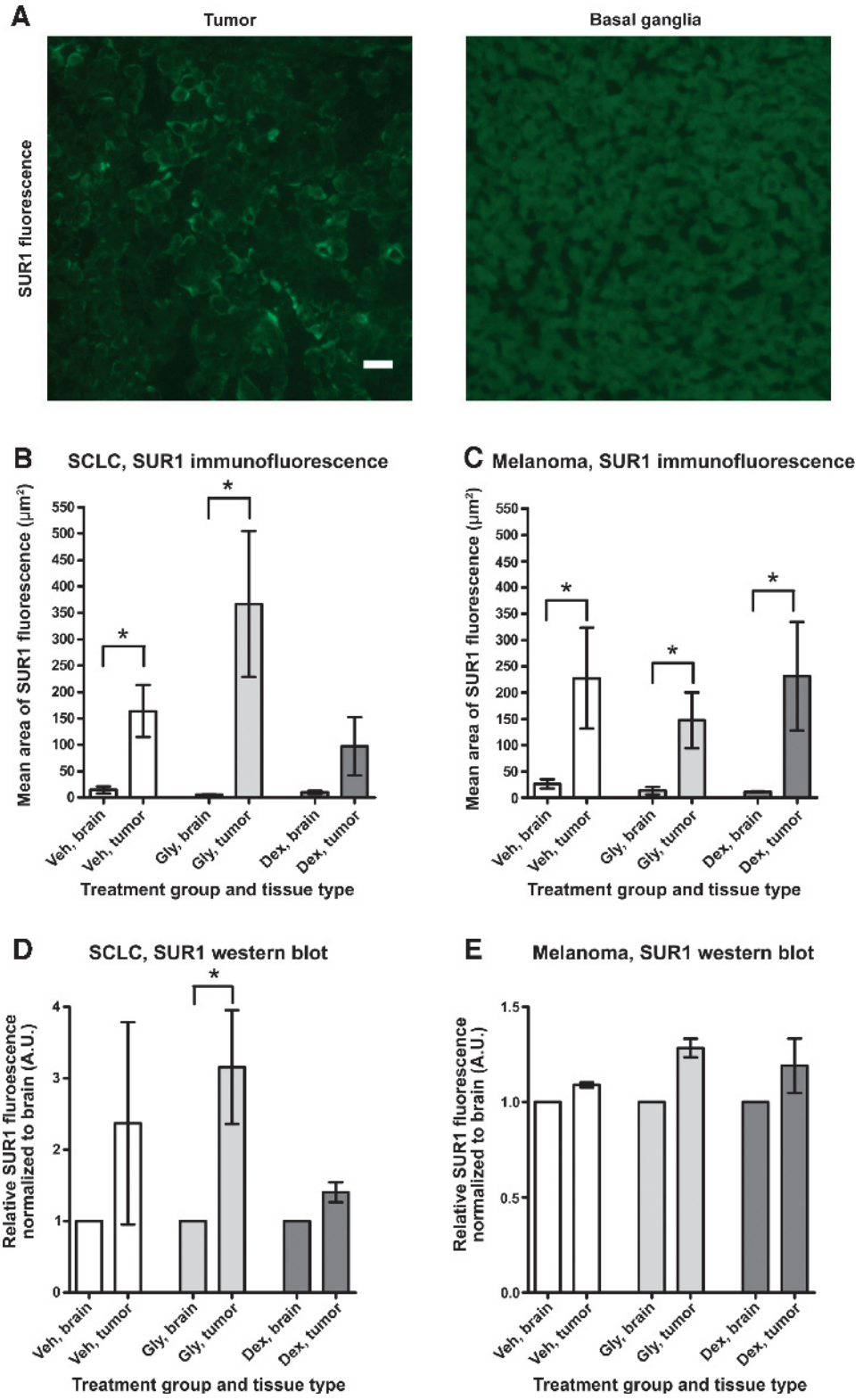

Figure 1. SUR1 is overexpressed in cerebral metastases. Representative histologic sections of a control animal with implanted SCLC LX1 cells (A, ×200) demonstrate robust SUR1 expression (fluorescent green) in glial cells compared to the contralateral BG with minimal constitutive expression. SUR1 expression is significantly higher in areas of cerebral SCLC (B) and melanoma (C) than contralateral BG as assessed by immunofluorescent staining. Western blots (D and E) also demonstrate increased SUR1 expression in tumoral regions. Bars are SEM. Scale bar, 20 μm. A.U., arbitrary units; Veh, vehicle; Gly, glyburide; Dex, dexamethasone, *$P < .05$.

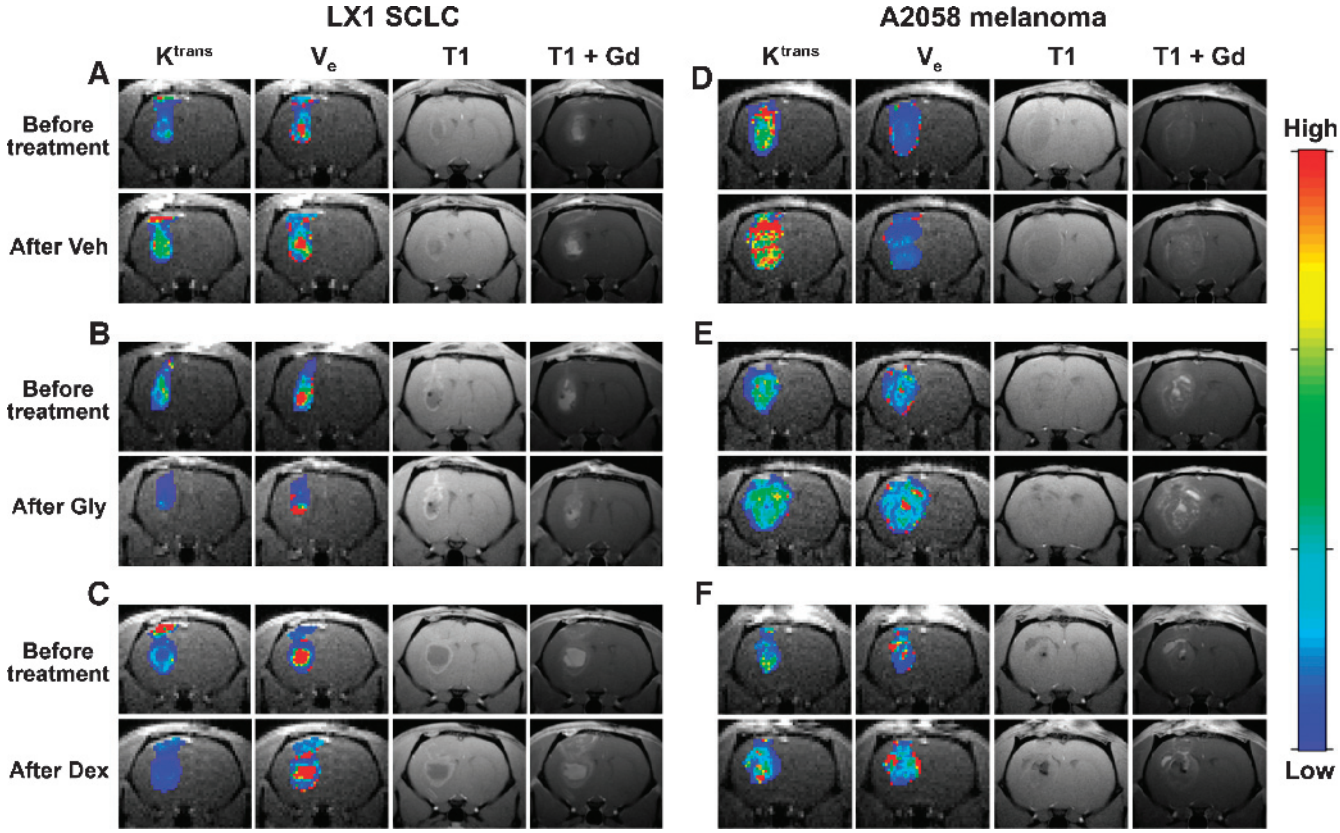

Figure 2. Glyburide and dexamethasone decrease permeability in cystic and solid tumors regardless of size but do not inhibit tumor growth. Representative coronal DCE and anatomic MR images from a single LX1 SCLC animal (A–C) in each treatment group before treatment and 48 hours later after treatment. Note the cystic nature of the SCLC tumors. Tumors in control animals (vehicle) demonstrate expected increased permeability as the tumor becomes larger (A). Administration of glyburide results in a decrease in K^{trans} and v_e (B). Administration of dexamethasone results in a decrease in K^{trans} and v_e (C). Representative coronal DCE and anatomic MR images from a single A2058 melanoma animal (D–F) in each treatment group before treatment and 48 hours later after treatment. Note the solid nature of the melanoma tumors and the large pretreatment size. Tumors in control animals demonstrate significant increase in K^{trans}, while v_e minimally increases as the tumor becomes larger (C). In contrast, administration of glyburide results in stable K^{trans} and v_e values despite tumor growth (D). Administration of dexamethasone limits increase of K^{trans}, while the v_e value in this animal increased (E). Veh, vehicle; Gly, glyburide; Dex, dexamethasone; Gd, gadodiamide.

SCLC and melanoma models as the tumor size increased (Figure 2, *A* and *D*). Following treatment, both glyburide and dexamethasone significantly decreased BTB permeability as determined by K^{trans} compared to controls in animals with SCLC ($P < .01$; Figures 2, *B* and *C*, and 3*A*). Glyburide significantly halted BTB permeability increase compared to controls in animals with melanoma ($P < .05$; Figures 2*E* and 3*C*). Dexamethasone also limited BTB permeability increase (Figures 2*F* and 3*C*) compared to controls in animals with melanoma, but this difference was not statistically significant. Glyburide and dexamethasone did not significantly alter v_e (Figure 3, *B* and *D*).

In a pilot study analyzing the effect of glyburide on a malignant glioma model (UW28 cells), animals were treated with doses of glyburide up to 9.8 μg twice daily. In contrast to both cerebral metastasis models, inhibition of SUR1 failed to limit the increase in BTB permeability associated with tumor growth. Treatment with neither glyburide nor dexamethasone restricted increases in K^{trans} (mean ± SEM): 49.3 ± 22.2% in the vehicle group, 84.1 ± 38.3% in the glyburide group, and 79.7 ± 52.0% in the dexamethasone group. v_e also increased in all groups (mean ± SEM): 136.9 ± 69.7% in the vehicle group, 23.93 ± 49.3% in the glyburide group, and 118.1 ± 98.4% in the dexamethasone group. This arm of the study was terminated due to treatment futility. Of note, no animal that received 9.8 μg of glyburide twice daily had serum blood glucose levels < 100 mg/dl.

SUR1 and Dexamethasone Decrease Tumor-Induced ZO-1 Gap Formation

Both hypoxia and inflammation, microenvironments found in tumors [29], rearrange and create gaps in ZO-1 at the blood-brain barrier [19,30]. Because inhibition of SUR1 has been linked to the rearrangement of ZO-1 in inflammation [19], we sought to explore the relationship of SUR1 and ZO-1 in metastatic tumors.

Animals in both metastatic models treated with glyburide or dexamethasone had significantly less ZO-1 gap distances compared to controls ($P < .01$; Figure 4, *A*–*C*). In some cases, SUR1 was expressed in the endothelial cells of vessels, co-localized with ZO-1 (Figure 4*D*). Notably, the expression of ZO-1 was not decreased by the presence of tumor when compared to contralateral BG (data not shown).

Decreased Tumor Vessel Permeability Does Not Correlate with Survival

In both metastatic models in all three treatment groups, tumor area increased in the 48 hours between the two DCE-MRI sessions ($P >$

.05). As a result, we found no difference in median overall survival between the three treatment groups in the SCLC model: vehicle (16 days), glyburide (16 days), and dexamethasone (16.5 days) (P = .735). There was a trend (P = .266) favoring increased survival in the glyburide group in the melanoma model: vehicle (14 days), glyburide (16.5 days), and dexamethasone (15 days). The rapid tumor growth in these aggressive tumor models likely confounded any potential difference in survival conferred by decreasing vasogenic edema. As glyburide is unlikely to have any direct cytotoxic effect on brain tumors, its clinical benefit will likely result from edema reduction and subsequent quality of life improvement, not survival prolongation.

Discussion

We demonstrated for the first time that SUR1 is overexpressed in SCLC and melanoma cerebral metastases. We also established that glyburide is at least as effective as dexamethasone at decreasing BTB permeability in cerebral metastases. This finding was validated using both negative (vehicle) and positive (dexamethasone) controls for BTB permeability and held true in both cystic tumors (SCLC) and solid tumors (melanoma). Further, we found that the decrease in permeability conferred by both glyburide and dexamethasone is at least in part due to decreased tumor-induced ZO-1 gap formation.

The Role of SUR1 Inhibition in Malignant Brain Tumors

Although Simard and colleagues have explored the role of SUR1 in stroke [17], traumatic brain injury (TBI) [18], spinal cord injury (SCI) [31], and SAH [19], SUR1 has not been reported as a mechanism for the formation of vasogenic edema in cerebral metastases. In a malignant glioma model, glyburide (5 μg/kg/min for 15 minutes) decreased the permeability conferred by monoxidil sulfate; however, no decrease in permeability was found with glyburide administration alone [32]. We found similar results in a pilot study using a UW28 malignant glioma model in which neither glyburide nor dexamethasone decreased BTB permeability when given in amounts analogous to human doses. This suggests that the mechanistic underpinning of tumor-induced cerebral vasogenic edema differs in primary malignant tumors and metastatic tumors and has important clinical implications. First, glyburide may be an alternative to dexamethasone for the treatment of metastatic cerebral tumors but may not be efficacious in malignant gliomas. Second, higher doses of dexamethasone may be required to treat

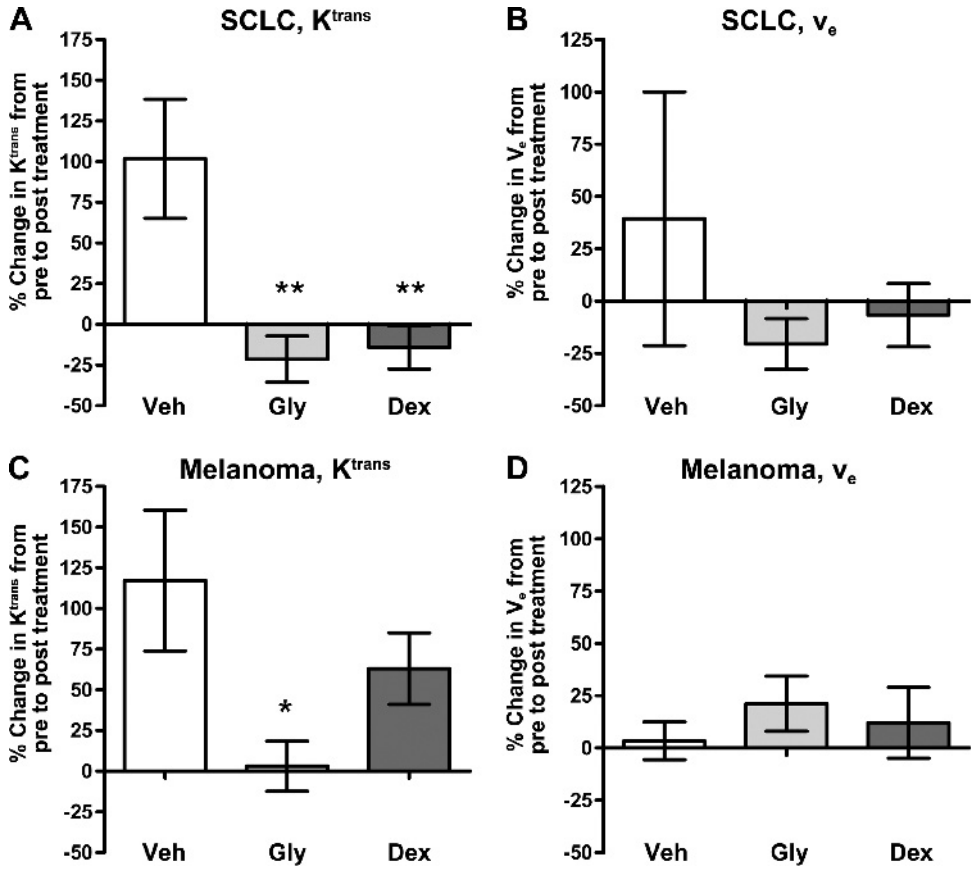

Figure 3. Inhibition of SUR1 by glyburide decreases BTB permeability in SCLC and melanoma metastases. Animals with SCLC cerebral metastases that received glyburide (mean K^{trans} change ± standard error, −21.4 ± 14.2%) or dexamethasone (−14.2 ± 13.1%) had a significant decrease in BTB permeability compared to controls (101.8 ± 36.6%) (A). Animals with melanoma cerebral metastases that received glyburide had significantly less BTB permeability increase (3.2 ± 15.4%) compared to controls (117.1 ± 43.4%) (C). Dexamethasone also lessened the permeability increase (63.1 ± 22.1%) compared to controls, but this did not reach statistical significance (C). Glyburide or dexamethasone did not significantly affect v_e in either metastatic model (B, D). Data are presented as the mean of six animals per group. Bars represent SEM. Veh, vehicle; Gly, glyburide; Dex, dexamethasone; $^{**}P < .01$, $^{*}P < .05$.

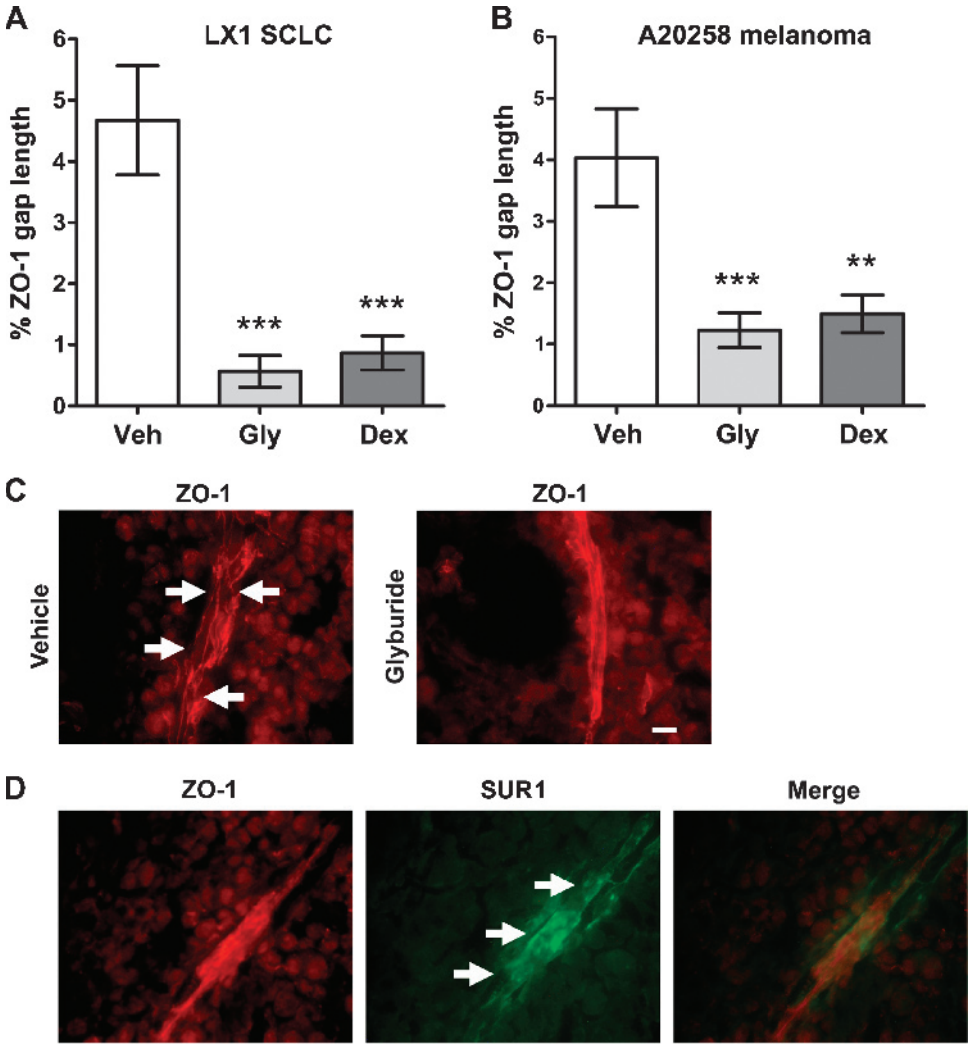

Figure 4. Glyburide and dexamethasone decrease BTB permeability by preserving ZO-1 at endothelial cell tight junctions. Both glyburide and dexamethasone administration result in significantly fewer and shorter gaps in ZO-1 compared to control animals that received vehicle in both SCLC (A) and melanoma (B) models. Representative immunofluorescent sections (C, ×400) of melanoma cerebral metastases in animals that received vehicle or glyburide. Note the continuous staining of ZO-1 in the glyburide-treated animal and the presence of multiple gaps (arrows) in ZO-1 staining in the vehicle-treated group. Representative histologic sections (D, ×400) of a control animal implanted with A2058 melanoma cells with immunofluorescent SUR1 staining in the intratumoral endothelial cells (arrows) co-localizing with ZO-1 expression. Veh, vehicle; Gly, glyburide; Dex, dexamethasone; $^{**}P < .01$, $^{***}P < .001$. Scale bar, 20 μm.

glioma-related edema compared to metastasis-related edema. Our group previously demonstrated this concept in which 2 mg/kg dexamethasone effectively decreased BTB in a malignant glioma model [12]. In contrast, a dose of 0.34 mg/kg in this study effectively decreased BTB permeability in SCLC cerebral metastases but not in malignant glioma. Future work will explore the intrinsic differences in BTB disruption between primary malignant and metastatic brain tumors.

ZO-1 Preservation in Brain Tumors

SUR1 has been shown to be overexpressed in animal models of inflammation due to SAH, which lead to ZO-1 rearrangement [19]. This presents a putative mechanism for the decrease of vasogenic edema by the inhibition of SUR1 with glyburide. Although both glyburide and dexamethasone administration correlated with a reduction in tumor-induced ZO-1 gaps, pathways to this end are likely different. We hypothesize that in cerebral metastases, glyburide blocks SUR1 in the endothelial cells, which likely prevents a cascade of cytotoxic edema [31], disruption of the actin cytoskeleton and ZO-1 at the tight junctions [33], and vasogenic edema. Glucocorticoids downregulate VEGF [7,8], which prevents the VEGF-induced decrease in ZO-1 expression [34,35]. Given their different mechanisms, future studies will determine if there is a synergistic relationship between glyburide and dexamethasone in the preservation of ZO-1 integrity in the BTB. Notably, in both models, we found no decrease in ZO-1 expression in areas of tumor, only increases in ZO-1 gaps in the control groups.

Glyburide versus *Dexamethasone*

The dose of glyburide used in this study, the equivalent of 2.5 mg/day in a 70-kg patient, is well tolerated in humans with mild hypoglycemia as the most common side effect [20]. In our study, no adverse events were related to glyburide administration. In contrast, almost 50% of patients treated with glucocorticoids develop deficiencies in

glucose metabolism, and in nearly half of these patients, disturbances persist despite reduction or even withdrawal of the drug [36]. Other common adverse effects of dexamethasone include hyperglycemia, peripheral edema, psychiatric disorders, immunosuppression, Cushing's syndrome, muscular weakness, femoral avascular necrosis, and pulmonary embolus [10]. A 1 month supply of dexamethasone is approximately $22 [37]. Given the multitude of adverse effects with prolonged dexamethasone use and the extraordinary expense of anti-VEGF antibodies at approximately $9000 per month [15], glyburide, a generic medication, may be an effective alternative to these agents for the treatment of vasogenic edema at $30 monthly [38]. The modest price of glyburide makes it amenable for widespread use in regions with limited financial resources.

Assessing Brain Tumor Permeability Therapeutics

DCE-MRI, the method used to determine cerebral vasculature permeability in this study, is arguably the most sophisticated way to measure BTB permeability in humans. Preclinical studies that have compared DCE-MRI *versus* quantitative autoradiography as a measurement of vasculature permeability in tumor [39] and stroke models [32] suggest that the two correlate extraordinarily well. However, DCE-MRI has the distinct advantage of comparing permeability within a single subject at multiple time points. We found that both glyburide and dexamethasone decreased BTB permeability as measured by K^{trans}, whereas these two agents did not seem to effect v_e. Since its inception, K^{trans} has been the gold standard for determining brain tumor permeably to which other methods are compared [40–42]. K^{trans} has also shown to be the permeability measure with the strongest correlation of glioma [43] and breast cancer grade [44]. Future studies will be conducted to determine the clinical relevance of v_e.

Limitations

Despite a decrease in BTB permeability, animals that received glyburide or dexamethasone did not survive significantly longer than controls. As expected, neither agent inhibited tumor growth. The lack of survival prolongation was likely due to the aggressive growth characteristics of both LX1 and A2058 tumors with median survival ranging from 14 to 16.5 days following tumor implantation. It is also possible that treatment with glyburide or dexamethasone was commenced too late to have a clinical effect. In humans with stroke, glyburide improved functional outcome [45] (although that finding is controversial [46]), but survival was not assessed. Future studies using less aggressive cell types and neurofunctional assessment are needed to determine the true clinical significance of decreased BTB permeability. It is certainly possible that decreasing BTB permeability with glyburide may benefit patients by reducing neurologic deficits associated with edema-related mass effect without improving survival.

No animal in this study experienced hypoglycemia in doses up to 9.8 μg twice daily. However, rats eat almost continually while awake, thus not replicating a typical human pattern of food consumption. Hypoglycemia must therefore be closely monitored in the initial treatment of patients with otherwise normal serum glucose.

In conclusion, SUR1 is overexpressed in SCLC and melanoma cerebral metastases. Overexpression of SUR1 may be one of the key mechanisms underlying cerebral metastatic tumor–related vasogenic edema. The safe and inexpensive SUR1 inhibitor, glyburide, is at least as effective as dexamethasone at decreasing BTB permeability in cerebral metastases. The decrease in permeability conferred by glyburide and dexamethasone is likely due to the decreased formation of tumor-induced gaps in the endothelial cell tight junction protein, ZO-1. This is a key mechanistic finding to explain the effect of these medications on BTB permeability.

The results of this work together with a long record of safe glyburide use in humans support a clinical trial to assess the ability of glyburide to decrease permeability as assessed by DCE-MRI and to investigate its effects on cognitive and motor outcomes. Glyburide may be a viable alternative to dexamethasone for the treatment of metastatic tumor–related vasogenic edema. With minimal cost and side effects, glyburide has the real potential to substantially improve quality of life in patients with cerebral metastases.

Acknowledgments

The authors thank Andy Rekito, MS, for figure preparation, Shirley McCartney, PhD, for editorial assistance, and Lindsay Reese, PhD, for Western blot assistance.

References

[1] Eichler AF, Chung E, Kodack DP, Loeffler JS, Fukumura D, and Jain RK (2011). The biology of brain metastases—translation to new therapies. *Nat Rev Clin Oncol* **8**, 344–356.

[2] Dolecek TA, Propp JM, Stroup NE, and Kruchko C (2012). CBTRUS statistical report: primary brain and central nervous system tumors diagnosed in the United States in 2005–2009. *Neuro Oncol* **14**, 1–49.

[3] Ortuzar W, Hanna N, Pennella E, Peng G, Langer C, Monberg M, and Scagliotti G (2012). Brain metastases as the primary site of relapse in two randomized phase III pemetrexed trials in advanced non–small-cell lung cancer. *Clin Lung Cancer* **13**, 24–30.

[4] Sharma M and Abraham J (2007). CNS metastasis in primary breast cancer. *Expert Rev Anticancer Ther* **7**, 1561–1566.

[5] Gaudino S, Di Lella GM, Russo R, Lo Russo VS, Piludu F, Quaglio FR, Gualano MR, De Waure C, and Colosimo C (2012). Magnetic resonance imaging of solitary brain metastases: main findings of nonmorphological sequences. *Radiol Med* **117**, 1225–1241.

[6] Andersen C and Jensen FT (1998). Differences in blood-tumour-barrier leakage of human intracranial tumours: quantitative monitoring of vasogenic oedema and its response to glucocorticoid treatment. *Acta Neurochir (Wien)* **140**, 919–924.

[7] Gerstner ER, Duda DG, di Tomaso E, Ryg PA, Loeffler JS, Sorensen AG, Ivy P, Jain RK, and Batchelor TT (2009). VEGF inhibitors in the treatment of cerebral edema in patients with brain cancer. *Nat Rev Clin Oncol* **6**, 229–236.

[8] Heiss JD, Papavassiliou E, Merrill MJ, Nieman L, Knightly JJ, Walbridge S, Edwards NA, and Oldfield EH (1996). Mechanism of dexamethasone suppression of brain tumor-associated vascular permeability in rats. Involvement of the glucocorticoid receptor and vascular permeability factor. *J Clin Invest* **98**, 1400–1408.

[9] Piette C, Munaut C, Foidart JM, and Deprez M (2006). Treating gliomas with glucocorticoids: from bedside to bench. *Acta Neuropathol* **112**, 651–664.

[10] Vecht CJ, Hovestadt A, Verbiest HB, van Vliet JJ, and van Putten WL (1994). Dose-effect relationship of dexamethasone on Karnofsky performance in metastatic brain tumors: a randomized study of doses of 4, 8, and 16 mg per day. *Neurology* **44**, 675–680.

[11] Muldoon LL, Gahramanov S, Li X, Marshall DJ, Kraemer DF, and Neuwelt EA (2011). Dynamic magnetic resonance imaging assessment of vascular targeting agent effects in rat intracerebral tumor models. *Neuro Oncol* **13**, 51–60.

[12] Varallyay CG, Muldoon LL, Gahramanov S, Wu YJ, Goodman JA, Li X, Pike MM, and Neuwelt EA (2009). Dynamic MRI using iron oxide nanoparticles to assess early vascular effects of antiangiogenic versus corticosteroid treatment in a glioma model. *J Cereb Blood Flow Metab* **29**, 853–860.

[13] Thompson EM, Dosa E, Kraemer DF, and Neuwelt EA (2010). Treatment with bevacizumab plus carboplatin for recurrent malignant glioma. *Neurosurgery* **67**, 87–93.

[14] Vredenburgh JJ, Desjardins A, Herndon JE II, Marcello J, Reardon DA, Quinn JA, Rich JN, Sathornsumetee S, Gururangan S, Sampson J, et al. (2007).

Bevacizumab plus irinotecan in recurrent glioblastoma multiforme. *J Clin Oncol* **25**, 4722–4729.

[15] Omuro AM and Delattre JY (2008). What is the place of bevacizumab and irinotecan in the treatment of glioblastoma and other malignant gliomas? *Curr Opin Neurol* **21**, 717–719.

[16] Chen M, Dong Y, and Simard JM (2003). Functional coupling between sulfonylurea receptor type 1 and a nonselective cation channel in reactive astrocytes from adult rat brain. *J Neurosci* **23**, 8568–8577.

[17] Simard JM, Chen M, Tarasov KV, Bhatta S, Ivanova S, Melnitchenko L, Tsymbalyuk N, West GA, and Gerzanich V (2006). Newly expressed SUR1-regulated NC(Ca-ATP) channel mediates cerebral edema after ischemic stroke. *Nat Med* **12**, 433–440.

[18] Simard JM, Kilbourne M, Tsymbalyuk O, Tosun C, Caridi J, Ivanova S, Keledjian K, Bochicchio G, and Gerzanich V (2009). Key role of sulfonylurea receptor 1 in progressive secondary hemorrhage after brain contusion. *J Neurotrauma* **26**, 2257–2267.

[19] Simard JM, Geng Z, Woo SK, Ivanova S, Tosun C, Melnichenko L, and Gerzanich V (2009). Glibenclamide reduces inflammation, vasogenic edema, and caspase-3 activation after subarachnoid hemorrhage. *J Cereb Blood Flow Metab* **29**, 317–330.

[20] U.S. Food and Drug Administration (2008). Micronase - glyburide tablet, September 2008 update. Available at: http://www.accessdata.fda.gov/drugsatfda_docs/label/2008/017498s027lbl.pdf.

[21] Haroon HA, Buckley DL, Patankar TA, Dow GR, Rutherford SA, Baleriaux D, and Jackson A (2004). A comparison of K^{trans} measurements obtained with conventional and first pass pharmacokinetic models in human gliomas. *J Magn Reson Imaging* **19**, 527–536.

[22] Patankar TF, Haroon HA, Mills SJ, Baleriaux D, Buckley DL, Parker GJ, and Jackson A (2005). Is volume transfer coefficient (K^{trans}) related to histologic grade in human gliomas? *AJNR Am J Neuroradiol* **26**, 2455–2465.

[23] Mills SJ, Soh C, Rose CJ, Cheung S, Zhao S, Parker GJ, and Jackson A (2010). Candidate biomarkers of extravascular extracellular space: a direct comparison of apparent diffusion coefficient and dynamic contrast-enhanced MR imaging—derived measurement of the volume of the extravascular extracellular space in glioblastoma multiforme. *AJNR Am J Neuroradiol* **31**, 549–553.

[24] Li X, Rooney WD, Varallyay CG, Gahramanov S, Muldoon LL, Goodman JA, Tagge IJ, Selzer AH, Pike MM, Neuwelt EA, et al. (2010). Dynamic-contrast-enhanced-MRI with extravasating contrast reagent: rat cerebral glioma blood volume determination. *J Magn Reson* **206**, 190–199.

[25] Tofts PS, Brix G, Buckley DL, Evelhoch JL, Henderson E, Knopp MV, Larsson HB, Lee TY, Mayr NA, Parker GJ, et al. (1999). Estimating kinetic parameters from dynamic contrast-enhanced T_1-weighted MRI of a diffusable tracer: standardized quantities and symbols. *J Magn Reson Imaging* **10**, 223–232.

[26] Woltjer RL, Nghiem W, Maezawa I, Milatovic D, Vaisar T, Montine KS, and Montine TJ (2005). Role of glutathione in intracellular amyloid-α precursor protein/carboxy-terminal fragment aggregation and associated cytotoxicity. *J Neurochem* **93**, 1047–1056.

[27] Karschin C, Ecke C, Ashcroft FM, and Karschin A (1997). Overlapping distribution of K_{ATP} channel-forming Kir6.2 subunit and the sulfonylurea receptor SUR1 in rodent brain. *FEBS Lett* **401**, 59–64.

[28] Suckow MA, Weisbroth SH, and Franklin CL (2006). *The Laboratory Rat*. Elsevier Academic Press, Burlington, MA.

[29] Schiffer D, Annovazzi L, Caldera V, and Mellai M (2010). On the origin and growth of gliomas. *Anticancer Res* **30**, 1977–1998.

[30] Bauer AT, Burgers HF, Rabie T, and Marti HH (2010). Matrix metalloproteinase-9 mediates hypoxia-induced vascular leakage in the brain via tight junction rearrangement. *J Cereb Blood Flow Metab* **30**, 837–848.

[31] Simard JM, Tsymbalyuk O, Ivanov A, Ivanova S, Bhatta S, Geng Z, Woo SK, and Gerzanich V (2007). Endothelial sulfonylurea receptor 1–regulated NC Ca-ATP channels mediate progressive hemorrhagic necrosis following spinal cord injury. *J Clin Invest* **117**, 2105–2113.

[32] Ningaraj NS, Rao MK, and Black KL (2003). Adenosine 5′-triphosphate-sensitive potassium channel-mediated blood-brain tumor barrier permeability increase in a rat brain tumor model. *Cancer Res* **63**, 8899–8911.

[33] Simard JM, Kahle KT, and Gerzanich V (2010). Molecular mechanisms of microvascular failure in central nervous system injury—synergistic roles of NKCC1 and SUR1/TRPM4. *J Neurosurg* **113**, 622–629.

[34] Wang W, Dentler WL, and Borchardt RT (2001). VEGF increases BMEC monolayer permeability by affecting occludin expression and tight junction assembly. *Am J Physiol Heart Circ Physiol* **280**, H434–H440.

[35] Ghassemifar R, Lai CM, and Rakoczy PE (2006). VEGF differentially regulates transcription and translation of ZO-$1\alpha^+$ and ZO-$1\alpha^-$ and mediates trans-epithelial resistance in cultured endothelial and epithelial cells. *Cell Tissue Res* **323**, 117–125.

[36] Meyer G and Badenhoop K (2003). Glucocorticoid-induced insulin resistance and diabetes mellitus. Receptor-, postreceptor mechanisms, local cortisol action, and new aspects of antidiabetic therapy. *Med Klin (Munich)* **98**, 266–270.

[37] Epocrates (2012). Dexamethasone. Available at: https://online.epocrates.com/noFrame/showPage.do?method=drugs&MonographId=189&ActiveSectionId=6.

[38] Epocrates (2012). DiaBeta, glyburide. Available at: https://online.epocrates.com/noFrame/showPage.do?method=drugs&MonographId=626.

[39] Ferrier MC, Sarin H, Fung SH, Schatlo B, Pluta RM, Gupta SN, Choyke PL, Oldfield EH, Thomasson D, and Butman JA (2007). Validation of dynamic contrast-enhanced magnetic resonance imaging-derived vascular permeability measurements using quantitative autoradiography in the RG2 rat brain tumor model. *Neoplasia* **9**, 546–555.

[40] Chu JP, Mak HK, Yau KK, Zhang L, Tsang J, Chan Q, and Ka-Kit Leung G (2012). Pilot study on evaluation of any correlation between MR perfusion (Ktrans) and diffusion (apparent diffusion coefficient) parameters in brain tumors at 3 Tesla. *Cancer Imaging* **12**, 1–6.

[41] Haris M, Husain N, Singh A, Awasthi R, Singh Rathore RK, Husain M, and Gupta RK (2008). Dynamic contrast-enhanced (DCE) derived transfer coefficient (ktrans) is a surrogate marker of matrix metalloproteinase 9 (MMP-9) expression in brain tuberculomas. *J Magn Reson Imaging* **28**, 588–597.

[42] Harrer JU, Parker GJ, Haroon HA, Buckley DL, Embelton K, Roberts C, Baleriaux D, and Jackson A (2004). Comparative study of methods for determining vascular permeability and blood volume in human gliomas. *J Magn Reson Imaging* **20**, 748–757.

[43] Law M, Young R, Babb J, Rad M, Sasaki T, Zagzag D, and Johnson G (2006). Comparing perfusion metrics obtained from a single compartment versus pharmacokinetic modeling methods using dynamic susceptibility contrast-enhanced perfusion MR imaging with glioma grade. *AJNR Am J Neuroradiol* **27**, 1975–1982.

[44] Radjenovic A, Dall BJ, Ridgway JP, and Smith MA (2008). Measurement of pharmacokinetic parameters in histologically graded invasive breast tumours using dynamic contrast-enhanced MRI. *Br J Radiol* **81**, 120–128.

[45] Kunte H, Schmidt S, Eliasziw M, del Zoppo GJ, Simard JM, Masuhr F, Weih M, and Dirnagl U (2007). Sulfonylureas improve outcome in patients with type 2 diabetes and acute ischemic stroke. *Stroke* **38**, 2526–2530.

[46] Favilla CG, Mullen MT, Ali M, Higgins P, and Kasner SE (2011). Sulfonylurea use before stroke does not influence outcome. *Stroke* **42**, 710–715.